DEPARTMENT OF THE INTERIOR

UNITED STATES GEOLOGICAL SURVEY

In Situ and Laboratory Geotechnical Tests in the Pierre Shale Near Hayes, South Dakota

By

Thomas C. Nichols, Jr.[1] and Donley S. Collins[1]

Open-File Report 86-152

This report is preliminary and has not been reviewed for conformity with U.S. Geological Survey editorial standards and stratigraphic nomenclature.

[1]U.S. Geological Survey
Denver, Colorado

1986

CONTENTS

ILLUSTRATIONS

TABLE

IN SITU AND LABORATORY GEOTECHNICAL TESTS IN THE PIERRE SHALE NEAR HAYES, SOUTH DAKOTA

By Thomas C. Nichols, Jr. and Donley S. Collins

ABSTRACT

A geotechnical investigation of the Pierre Shale near Hayes, S. Dak., was conducted by the U.S. Geological Survey. The physical and mechanical properties of the shale were determined through use of four core holes and several supplementary holes, drilled to a maximum depth of 184 m. In situ borehole determinations included a gravimeter survey, pressuremeter testing, thermal profile measurements, and borehole velocity measurements of shear and primary waves. Onsite laboratory measurements included geologic logging of cores, bulk density determinations, moisture content determinations, and rebound measurements. Offsite laboratory measurements included sonic velocity measurements of shear and primary waves, X-ray mineralogy and major element determinations, size analyses, fracture analyses, fabric analyses, and determination of thermal properties.

Below 15-22 m, the shale is an unweathered, saturated, overconsolidated, underpressured clay shale with a clay-mineral content ranging from 50 to 100 percent, dominantly composed of a mixed-layer of illitic smectites. The physical and mechanical properties, best determined by the in situ measurements vary widely, especially moisture contents, void ratios, and deformation moduli. Typically, microfractures occur throughout the shale with a low frequency except near larger fracture zones and at shallow depths just below the weathered zone. There are two large fracture zones at depth that contain no alteration products or extensive gauge developments indicative of large displacements. The thermal and mechanical properties change markedly when the shales desiccate.

The state of stress and overconsolidation appear to be functions of the depositional and erosional history of the deposit, and both are markedly affected by large fracture zones. Significant rebound creep deformations occur upon unloading.

INTRODUCTION

Most of the Cretaceous clay shale of North America occurs in the western half of the conterminous United States and of Canada. In the United States, these rocks either are exposed or underlie younger Cretaceous, Tertiary, or Quaternary deposits at shallow depths throughout most of the northern and central Great Plains province, the intermontane basins of the Rocky Mountain system, and the Colorado Plateaus province. The clay shales become thin to nonexistent in the eastern Dakotas and Nebraska, and generally thicken westward. In deeper parts of Cretaceous marine basins adjacent to the Rocky Mountains of Colorado, it exceeds a thickness of 2,440 m (Tourtelot, 1962). The shales are generally saturated, relatively poorly consolidated marine silt and clay deposits, usually containing large amounts of smectite (swelling clay). The deposits appear to be uniform and massive over broad areas, devoid of structural features other than local gravitational slumps, well-developed bedding planes, and occasional thin but extensive bentonite beds.

Because of their very widespread occurrence at and near the ground surface, the shale deposits are subject to extensive engineering development and usage. Although presently most of the outcropping shales occur in sparsely populated areas, there are several rapidly growing urban centers that may give rise to intense local engineering development within the shale terranes.

In an attempt to obtain a better understanding of the engineering characteristics of clay shales, especially those pertaining to long-term stability under the severe environmental conditions imposed by toxic wastes, the U.S. Geological Survey (USGS) has initiated a research program which includes geotechnical studies of the Pierre Shale in South Dakota.

This report describes the field and laboratory investigations that have been conducted thus far to provide geotechnical data needed for the studies.

ACKNOWLEDGMENTS

This report contains basic data obtained from investigations carried out by Woodward-Clyde Consultants, Thermophysical Properties Research Laboratory, and the University of Colorado, under contract to the USGS. Much of the in situ geotechnical data for the Pierre Shale could not have been obtained without the expertise of Robert Pemberton. The X-ray analyses were done by L. G. Schultz, and the in situ borehole density measurements were made by J. W. Schmoker.

FIELD AND LABORATORY INVESTIGATIONS

The field investigations were conducted about 48 km west of the State capitol, Pierre, near the town of Hayes, S. Dak. (fig. 1). The study area is located atop a broad plateau bounded by the Bad River drainage on the south, the Missouri River trench on the east, and the Cheyenne River on the north and west. The local topographic relief (fig. 1) is very low, being no more than 97.6 m within a radius of 8.9 km. The investigations were conducted entirely within the Elk Butte, Mobridge, Virgin Creek, Verendrye, and DeGrey members of the Upper Cretaceous Pierre Shale. As described by Crandell (1958), these five members of the Pierre Shale are underlain by the Crow Creek, Gregory, and Sharon Springs members. The Sharon Springs member is directly underlain by the Niobrara Formation. The known thickness of the Pierre Shale near the vicinity of the investigation ranges from 244 to 366 m. At the study area, the Elk Butte and Mobridge members of the Pierre Shale are mainly exposed at the surface and generally locally covered by thin colluvium and alluvium in stream valleys and soil horizons on the divides.

The data used for this investigation were obtained from eight holes drilled in the study area (fig. 1; table 1). Of these, four produced continuous core samples, whereas, the rest were used for in situ geophysical and geotechnical tests and selected core samples. The four core holes were cored to provide specific geotechnical and geologic information needed to fulfill the stated study objectives. Lithologic logs indicate that the base of coring in the deepest hole was within the DeGrey member of the Pierre Shale at 182 m.

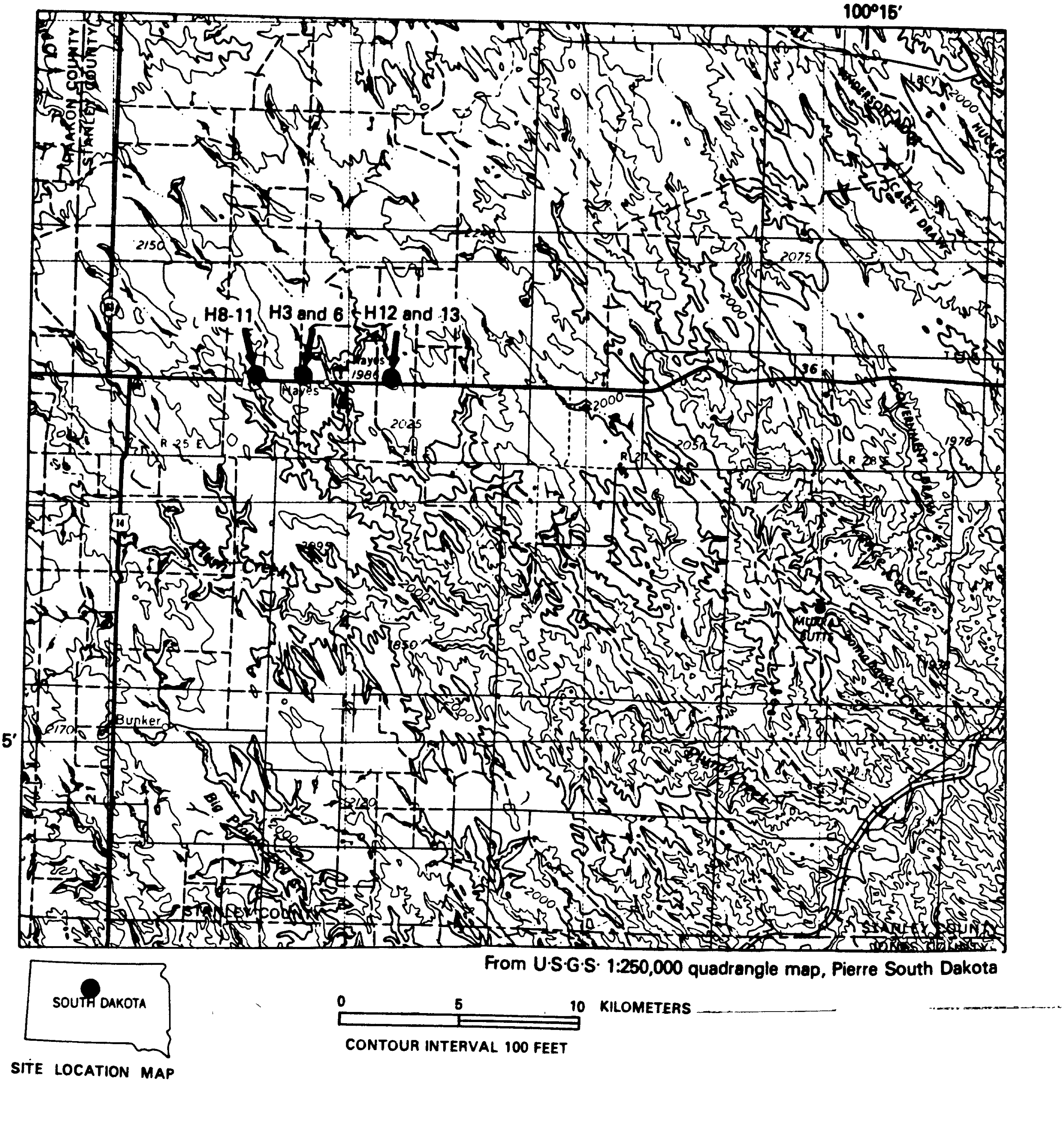

Figure 1.--Topographic map showing locations of drill sites near Hayes, S. Dak.

TABLE 1.--Descriptions of holes drilled for field study

Hole No.	Direction from Hayes (km)	Depth (m)	Purpose
H3	1.5 W.	184	Thermal measurements.
H6	1.5 W.	137	Borehole gravimeter measurements.
H8	3.0 W.	71	Core retrieval for geologic logs and physical-properties tests.
H9	3.0 W.	180	Uphole velocity measurements.
H10	3.0 W.	27	Core retrieval for geologic logs and physical-properties tests.
H11	3.0 W.	18	Do.
H12	2.5 E.	182	Do.
H13	2.5 E.	171	Pressuremeter measurements and selected core retrieval for logs.

Holes H8, H10, H11, and H12, respectively, 71, 27, 18, and 182 m deep, were used as core holes. Retrieved cores were logged for geologic features and core samples were selected approximately every 15 m for physical properties testing. Hole H3, 184 m deep, was used to make a thermal profile and heat-flow measurements (Sass and Galanis, 1983). H6, 137 m deep, was used for gravity measurements with a borehole gravimeter, and H9 was used for uphole velocity measurements of both shear and primary waves that were obtainable only to depths of about 30 and 90 m, respectively. H13, 171 m deep, was used for pressuremeter measurements.

The initial field effort was made to determine the in situ conditions, properties, and characteristic mechanical behavior of the bedrock. Because the Pierre Shale is softer than most rocks and mechanical behavior is easily changed through hydration, desiccation, and chemical alteration, great care was used in the selection of the methods used to obtain the most accurate geotechnical measurements. For instance, all boreholes were drilled dry, using air instead of drilling mud to remove cuttings, thereby leaving the borehole walls in a nearly undisturbed condition. The boreholes drilled in this manner yielded high-quality in situ geotechnical measurements.

Borehole measurements were made at regular intervals to obtain profiles of in situ density, thermal gradient, sonic velocities, elastic- and anelastic-deformation properties, to interpret existing and past stress conditions, and rebound potential. Other onsite laboratory measurements and observations were made on selected cores, immediately after being removed from boreholes, to determine natural-moisture content, bulk density, rebound response, lithology, and structure. Cores not used for onsite laboratory tests were wrapped in aluminum foil, sealed with wax, and stored for further laboratory testing or future reference.

Sealed cores returned to the USGS and commercial laboratories were tested for sonic velocities, grain specific gravities, continued rebound deformations, X-ray mineralogy, size analyses, chemical analyses, coefficient of thermal expansion, thermal conductivity, specific heat, three-dimensional consolidation, and deformation properties. In addition, rock fabric was examined by polarizing-microscopy and scanning electron-microscopy techniques.

RESULTS

Table 1 graphically presents a profile of the physical properties, natural thermal and mechanical loading conditions, and lithology of the shale below the weathered zone as determined from core holes H8 and H12 and drill holes H6, H9, and H13. The designations of depth for data presented in figure 2 are corrected to a common elevation datum plane of 640.2 m above mean sea level (the surface elevation of hole H12), which is taken as zero depth.

The H8 location is in an actively eroding valley approximately 5.8 km west and 15 m lower in elevation than the H12 location on a less actively eroding upland surface. If the bedding between the holes has approximately a flat dip as indicated by Crandell's (1958) mapping to the east, it is possible to correct the H8 and H12 profiles to the same elevation as shown in figure 2. Then cores sampled at equivalent elevations in each borehole may have similar lithology and properties. However, as lithologies and dips rarely remain constant even over short distances, the variance in lithology seen in figure 2 is not unexpected.

FRACTURES AND MICROFRACTURES

In columns 1 and 2 on plate 1, symbols represent geologic features (fractures and bentonite beds) observed in cores extracted from boreholes H8 and H12. The apparent base of the highly fractured chemical and mechanical weathered zone appears to be at shallower depths (9 m) in the more actively eroding valley environment (H8) than depths (22 m) at the less actively eroding divide locations (H12). Of some interest, however, is the fact that the elevation at the base of weathering in the valley environment is only 2 m lower than the base of weathering at the divide environment. This suggests the possibility that both zones had a common elevation prior to valley cutting. Perhaps the more important features affecting the geotechnical properties are the weathering, structural and depositional features; that is, weathered zone, fractures, faults, bedding-plane attitudes and soft-sediment deformations. Below the weathered zone, the character and distribution of fractures and faults within the shale are most significant to the in situ engineering behavior. Geologic logs compiled for cores from holes H8 and H12 show that most of the fractures not occurring in fracture zones are widely spaced and dip more than 45^{0}. All fractures are thin, discontinuous, localized features often terminating at other fracture surfaces or just disappearing within the core samples. Strikes of the fractures were not measurable because the horizontal orientation of the cores was not possible to determine. Fractures observed in cores from hole H12 had either flat to wavy-smooth surfaces or wavy-slickensided surfaces. Cores from 22 to 39 m contained five natural fractures with dips greater than 45^{0}, and three with

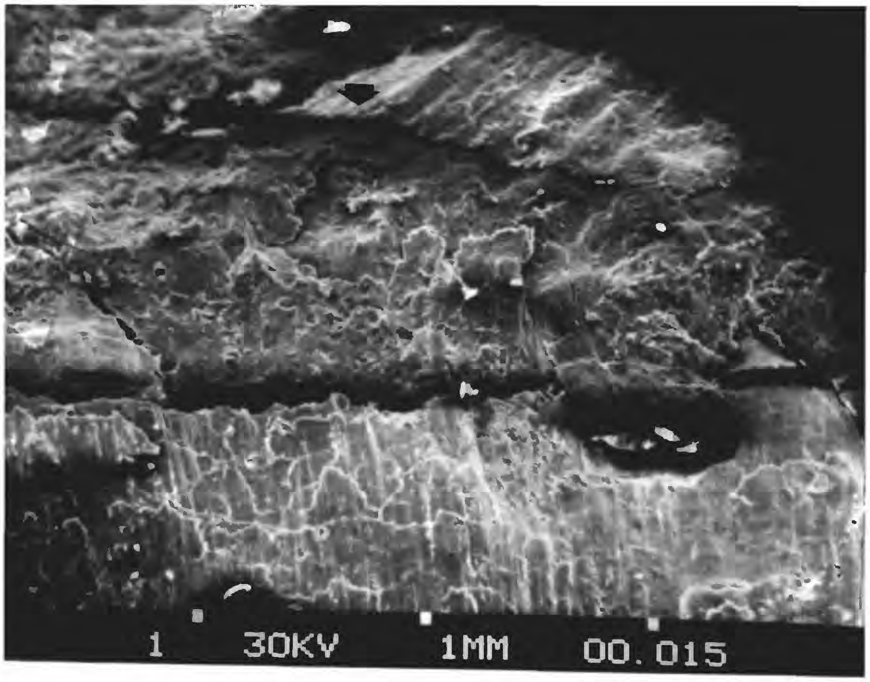

A

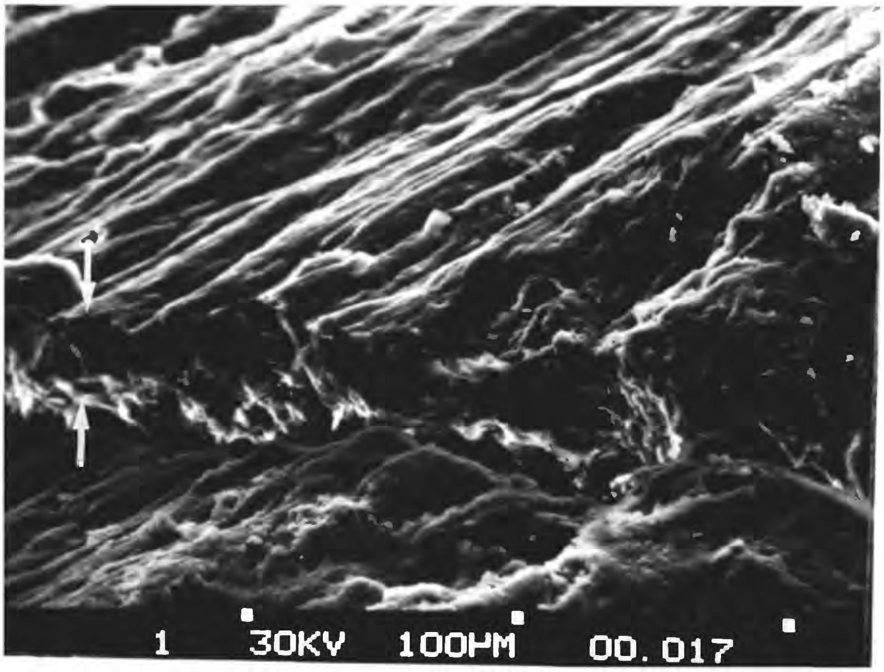

B

Figure 2.--SEM (scanning electron microscope) photographs of slickensided gouge sheets. Sample taken from hole H12 at 88.4-m depth. A, arrows show slickensided gouge covering fracture face. B, arrows show thickness of gouge.

dips less than 45^o. The fracture faces were mostly smooth surfaces, either flat or wavy, with fine coatings of clay particles. One fracture with a dip of 40^o had slickensides. From 39 to 70 m, no natural fractures were observed in cores.

Two fracture zones were observed between 70 and 92 m in which the observed fracture density significantly increases. A similar zone of increased fracture density between 32- and 39-m depth in hole H8 is equivalent in altitude to the 52- to 59-m depth in H12. Typically, these zones are on the order of 5 m thick and are characterized by increasing fracture density toward the center of each zone. The rock texture within the center of the zones is one of highly comminuted, nonaltered rock fragments as small as 0.25 cm across and with most of the fragments bounded by slickensided surfaces. Although the zones are highly fractured, the recovered fragmented shale lacked free water in fracture spaces and contained no evidence of chemical alteration or extensive gouge development indicative of large displacements. Based on drilling observations and laboratory data, there is no indication that the zones intersect a water table or the ground surface. Only thin (rarely exceeding several tens of microns thick) films of slickensided gouge were seen on the fracture surfaces of individual fragments (fig. 2). The true dips of the fracture zones are not known, but the location of these zones on the acoustic televiewer logs (F. Paillet, oral commun., 1984), in holes H12 and H12a (drilled for the USGS, only 12 m to the west of H12) and interval core logs from hole H13 (61 m east of H12), indicates the apparent dip of the two zones within 70-92 m is between 0^o and 17^o to the west on an east-west azimuth.

Microcracks were observed in all the thin sections made from the core samples selected every 15 m. Lower hemisphere projections of poles to microcracks for samples taken to depths of 170 m (not corrected to 640.2-m datum plane) are shown in figure 3. Most of the cracks observed are low density (less than 10 per section sweep), within 5^o of horizontal, and are approximately parallel the flat to shallow-dipping bedding planes. However, for unweathered shale at depths of 15-18 m in holes H10 and H11, the microfracture density increases significantly and the orientations of apparent dips (strikes not known), though basically low angle, tend to diverge from the horizontal bedding planes. At depths between 123 and 139 m in hole H12, a similar tendency is noted near or within the bentonite zones where bedding and soft sediment deformations occur at dips up to 22^o. Although most of the microcracks observed have been enhanced by the thin section preparation techniques, the occurrence of secondary mineralization on both sides of fracture boundaries implies that they are natural fractures.

TEXTURE AND MINERALOGY

The texture, mineralogy, and pore-water content are addressed in columns 3 through 11 on plate 1, on the basis of data from holes H6, H8, and H12. Included are: the percent of total clay minerals and mixed-layer clay minerals based on X-ray diffraction techniques, grain size, moisture content, void ratio, degree of saturation, carbonate content, and bulk density that were determined by in situ and laboratory testing techniques. These properties demonstrate that the Pierre Shale at these locations is a highly porous, low-density, saturated clay rock with a high content of mixed-layer

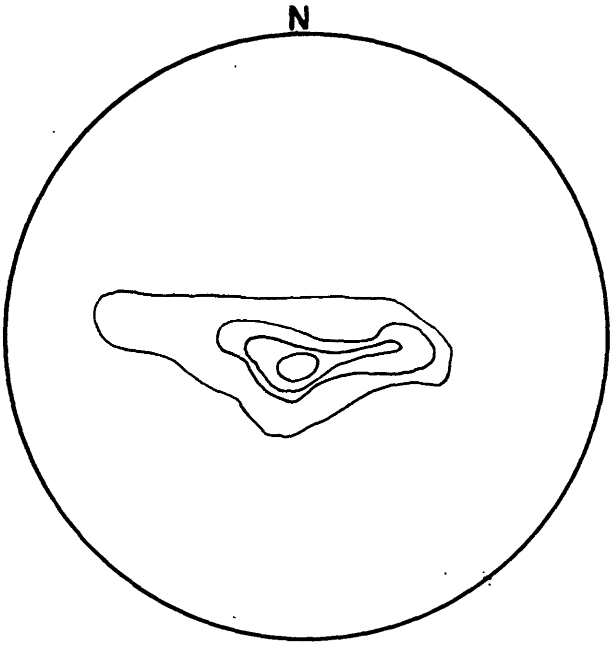

A. Percent contour areas are 0, 8.3, 16.6, 24.9, and 33.2
DEPH 16 m, HOLE H11

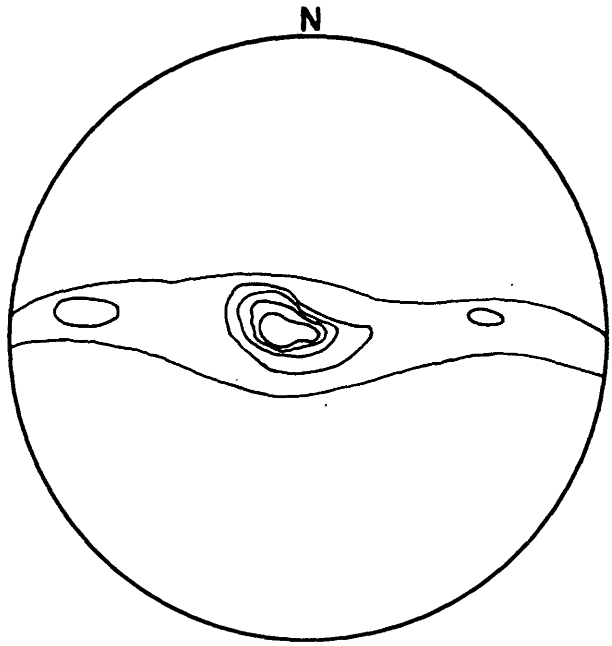

B. Percent contour areas are 0, 4.76, 9.52, 14.28, and 19.04
DEPTH 17m, HOLE H10

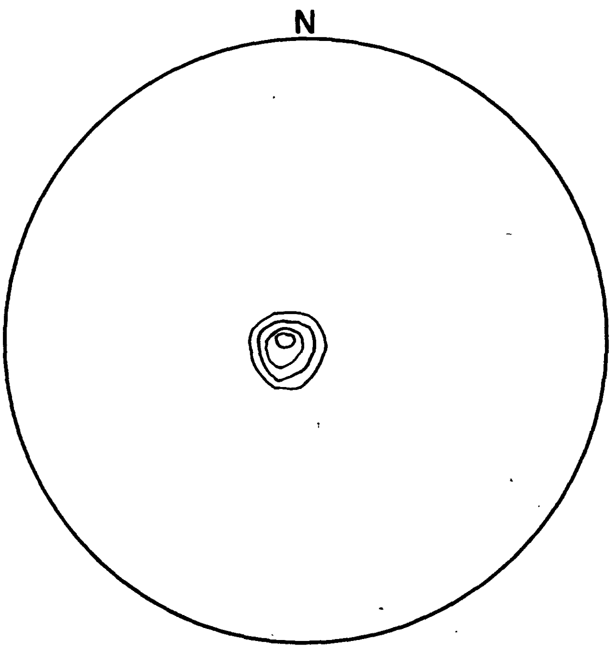

C. Percent contour areas are 25.0, 50.0, 75.0, and 100.0
DEPTH 23 m, HOLE H12

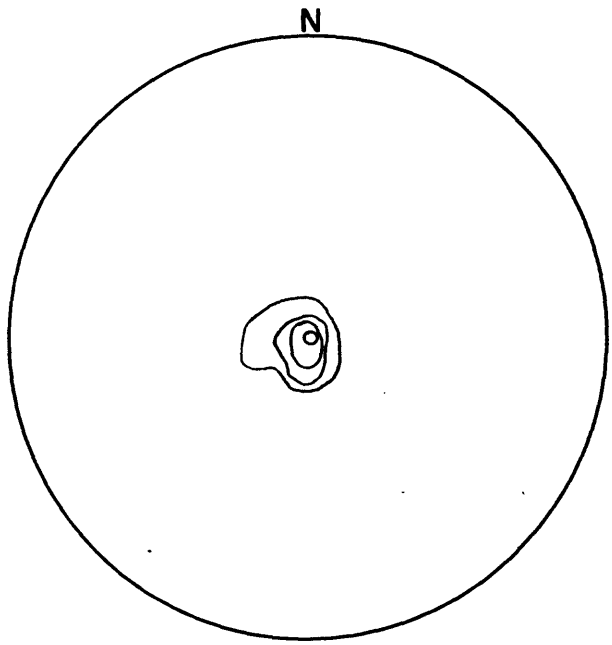

D. Percent contour areas are 20.0, 40.0, 60.0, and 80.0
DEPTH 48 m, HOLE H12

Figure 3.--Lower hemisphere equal-area plots of poles to microcracks determined in their sections from selected depths (not corrected to 640.2-m datum plane) in holes H10, H11, and H13.

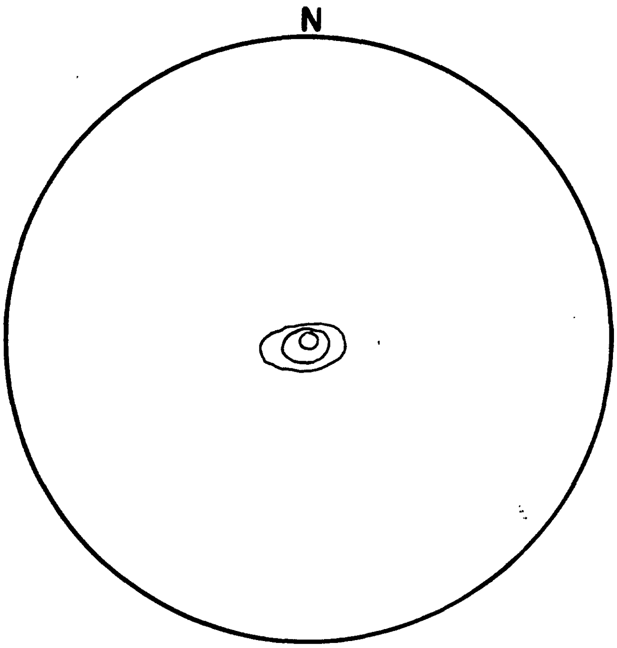

E. Percent contour areas are 16.67, 33.53, and 50.29
DEPTH 63 m, HOLE H12

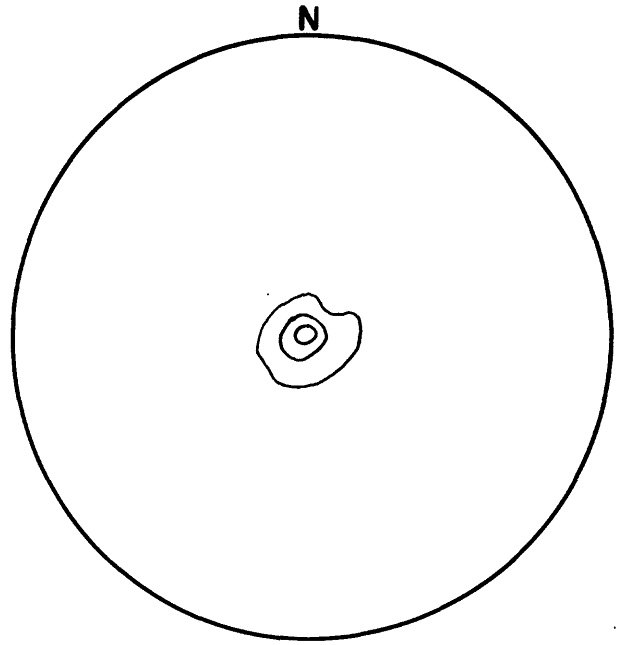

F. Percent contour areas are 12.5, 25.0, and 37.5
DEPTH 78 m, HOLE H12

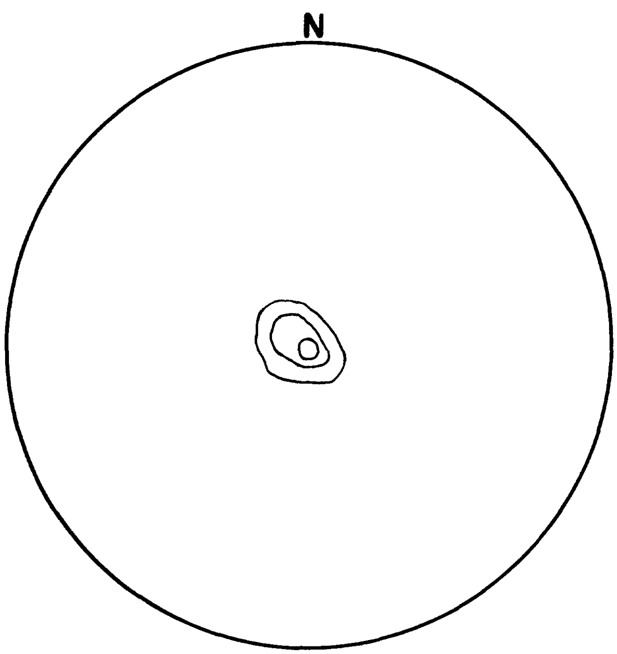

G. Percent contour areas are 33.33, 66.67, and 100.00
DEPTH 93 m, HOLE H12

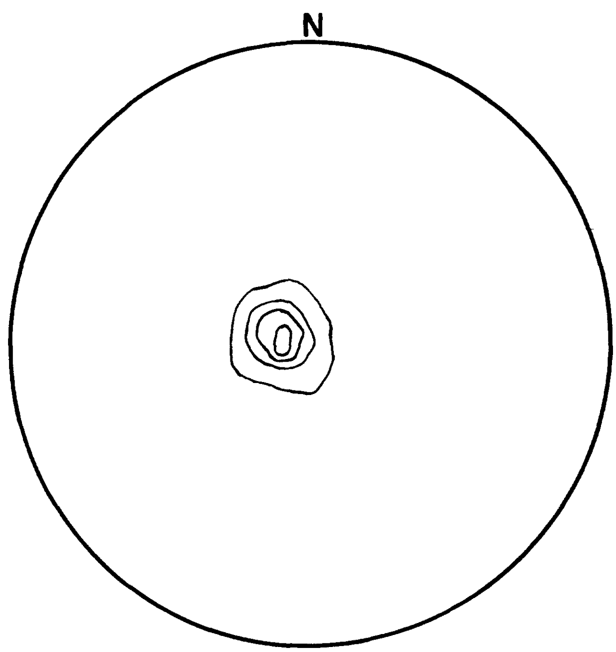

H. Percent contour areas are 0, 16.67, 33.33, and 50.01
DEPTH 109 m, HOLE H12

Figure 3.--Lower hemisphere equal-area plots of poles to microcracks determined in their sections from selected depths (not corrected to 640.2-m datum plane) in holes H10, H11, and H13--Continued

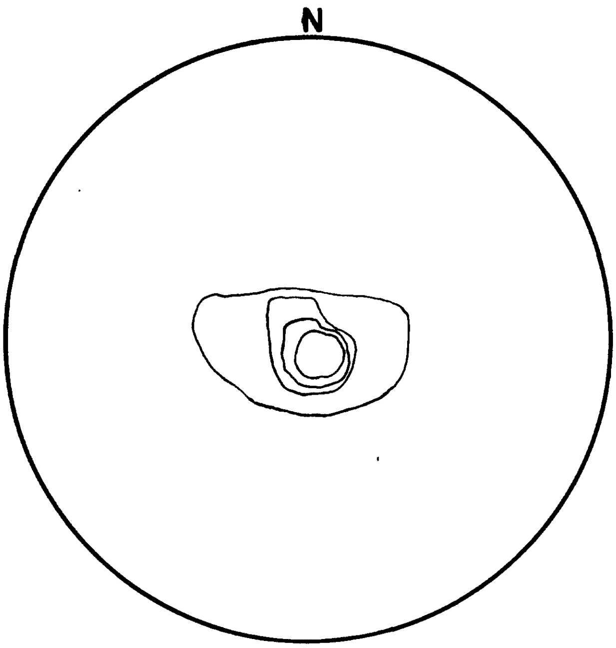

I. Percent contour areas are 0, 8.33, 16.67, and 33.33
DEPTH 123 m, HOLE H12

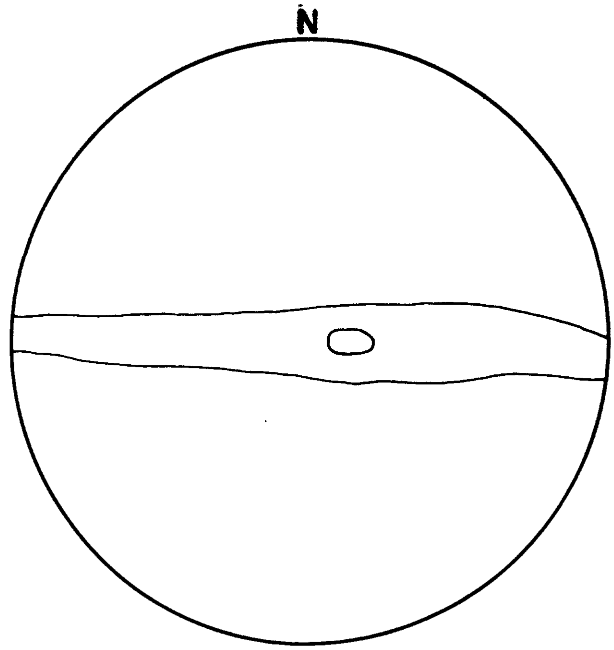

J. Percent contour areas are 16.67 and 33.33
DEPTH 139 m, HOLE H12

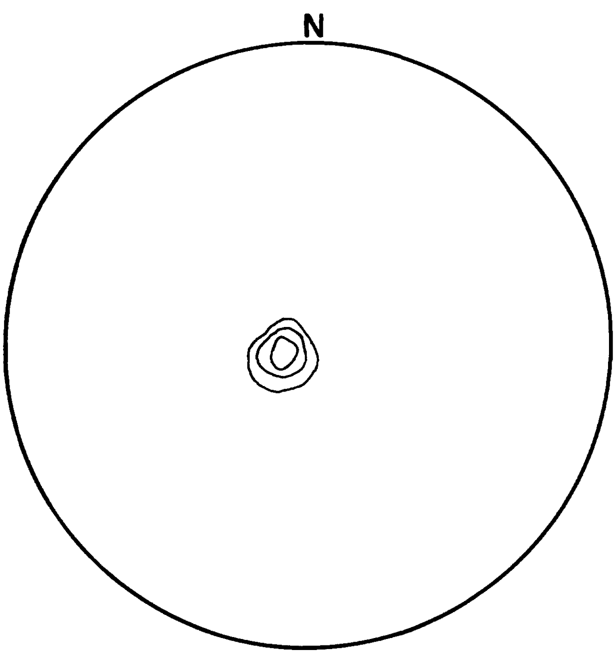

K. Percent contour areas are 33.33, 66.6, and 100.00
DEPTH 155 m, HOLE H12

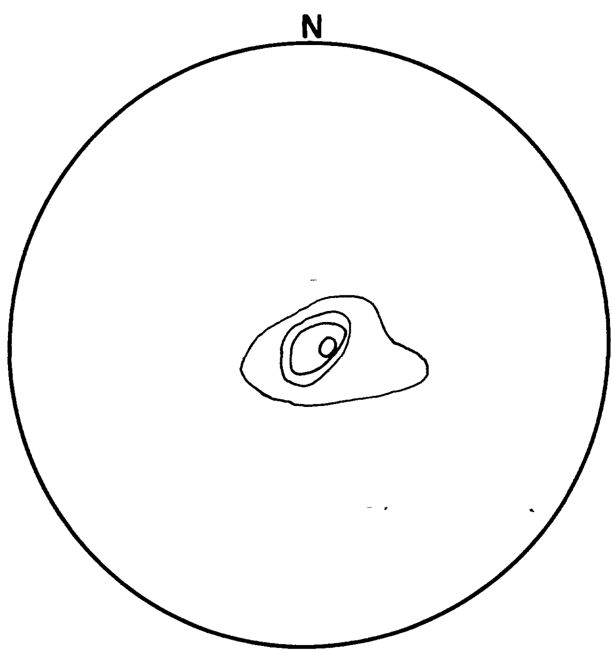

L. Percent contour areas are 10, 20, 30, and 40
DEPTH 170 m, HOLE H12

Figure 3.--Lower hemisphere equal-area plots of poles to microcracks determined in their sections from selected depths (not corrected to 640.2-m datum plane) in holes H10, H11, and H13--Continued

illitic smectites and numerous bentonite beds consisting totally of smectites (swelling clays). The material sampled to 61 m below the datum (pl. 1) in hole H8, however, appears to be consistently finer grained, slightly more clayey, more porous, less dense, containing more pore fluid, and having a slightly different mineral content than the material in hole H12 (pl. 1). The clay minerals in hole H8 appear to contain slightly more mixed-layer clays and the percentage of carbonates appears to be lower than those in hole H12.

In addition to bulk densities that were determined for holes H8 and H12 in the field laboratory, bulk densities were also determined with borehole gravimeter measurements in hole H6 (column 11, pl. 1). For the most part, the borehole gravimeter density values are somewhat greater than those determined in the field laboratory.

THERMAL GRADIENT

Columns 12 and 13 in plate 1 illustrate temperature- and thermal-gradient profiles measured in hole H3 (Sass and Galanis, 1983). The temperature profile does not appear to be affected by seasonal variations below 30 m. At 30 m, the rock temperature is approximately 12^{o} C and increases approximately 2.13 ^{o}C per 30 m with depth. At 178 m the temperature is about 22 ^{o}C. The thermal gradient in the lower 101 m is linear and approximately equals 2.06 ^{o}C per 30 m.

YOUNG'S MODULI

Columns 14 and 15 in plate 1 show profiles of static and sonic Young's moduli determined in situ and in the laboratory. Shown in column 14 are Young's moduli calculated from in situ vertical velocities measured in hole H10. Columns 14 and 15 in plate 1 show profiles of static and sonic Young's moduli determined in situ and in the laboratory. The Young's modulus profile calculated from laboratory-determined sonic velocities (pulse technique) in the horizontal and vertical directions of core samples from 15-m intervals in hole H12 are shown in column 15, plate 1. For the 152- and 169-m depths in hole H12, four data points show horizontal and vertical moduli determined from core velocity measurements made in five independent directions assuming a transverse anisotropy. The sonic moduli display three important variations: (1) the horizontal sonic moduli determined from all measurements are greater than the vertical moduli, indicating the shale to be stiffer in the horizontal plane; (2) the vertical and horizontal moduli determined for the transversely anisotropic case are lower than corresponding moduli determined for the respective directional velocities; and (3) the variations of sonic moduli with depth in hole H12 indicate significant changes in shale stiffness with depth.

Column 15, plate 1, includes profiles of static Young's moduli for holes H8 and H13. Undrained triaxial tests were conducted on cores from hole H8 (58-78 m corrected to the datum of plate 1) at room temperature, and lithostatic pressure at the University of Colorado under a constant strain rate (W. A. Braddock, oral commun., 1982). Measured strains and loads used to calculate the moduli were normal-to-nearly horizontal bedding. The static modulus profile shown for hole H13 was determined from undrained in situ horizontal measurements made with a Menard pressuremeter. The moduli are referred to as reload moduli (Davidson, 1979) and are determined using volumetric strain and pressure data obtained from the pressuremeter test.

In comparison with the laboratory-determined horizontal sonic moduli for hole H12, the in situ static moduli for hole H13 demonstrate similar but more pronounced variations of stiffness with depth. Since the pressuremeter determinations were made only in the horizontal directions, there are no vertical in situ static moduli for comparison to the laboratory-determined vertical static moduli for hole H8. However, the pressuremeter-determined horizontal moduli are mainly larger than the laboratory-determined vertical static moduli, which agrees with the similar comparison of horizontal-to-vertical sonic moduli. Finally, a comparison of static-to-sonic moduli reveals that the sonic moduli are almost always greater than the comparable static moduli, which is a well-known phenomenon reported profusely in the literature.

IN SITU STRESS AND OVERCONSOLIDATION RATIOS

The horizontal effective stresses were calculated from measurements made with a Menard pressuremeter in hole H13. Pore pressures were assumed to be approximately one-half of the hydrostatic pressure, on the basis of measurements made by Neuzil and Pollack (1983). The vertical effective stresses used for the determination of K_0 are calculated from average in situ specific gravities determined from the borehole gravimeter measurements (pl. 1). Profiles showing the state of stress and overconsolidation ratios (OCR = ratio of maximum past overburden to existing overburden) versus depth are presented in figure 4. Values of the coefficient of earth pressure at rest (ratio of horizontal-to-vertical stress, K_0) are shown at some data points. A plot of effective stress for $K_0=1$, the lithostatic condition, is superposed for comparison on the other curves, showing that the natural stress field appears to be almost lithostatic. As may be expected, examination of the stress profile shows a definite increase of the horizontal stress and a decrease of overconsolidation ratios with depth. However, the data indicate unexpected changes in both data curves between depths of 61 and 110 m (corrected to the datum in pl. 1), especially in the overconsolidation ratio curve where there is a definite break that occurs between the two large fracture zones.

THERMOMECHANICAL PROPERTIES

The thermomechanical properties measured in the laboratory include thermal expansion, specific heat, and conductivity determined on cores from hole H12. The thermal-expansion measurements were conducted at atmospheric pressure on selected natural-state cores (fig. 5) at temperatures ranging from 5^{o} to 25 ^{o}C, on drying core (fig. 6) from 19^{o} to 90 ^{o}C and on dry core (fig. 7) from 24^{o} to 210 ^{o}C. The specific-heat measurements (fig. 8) were made on samples partially predried at 110 ^{o}C in air. These were conducted in two successive runs on each sample under atmospheric pressures at temperatures from 42^{o} to 202 ^{o}C. Thermal-conductivity measurements (Sass and Galanis, 1983) were made at natural-moisture content and room temperature and pressure on selected cores from hole H8 taken 70-72 m depth below the 640.2-m datum plane. Six vertical values averaged 1.38 Wm^{-1} C^{-1} and six horizontal values averaged 1.28 $Wm^{-1}C^{-1}$, thus, showing slightly greater conductivity in the vertical direction.

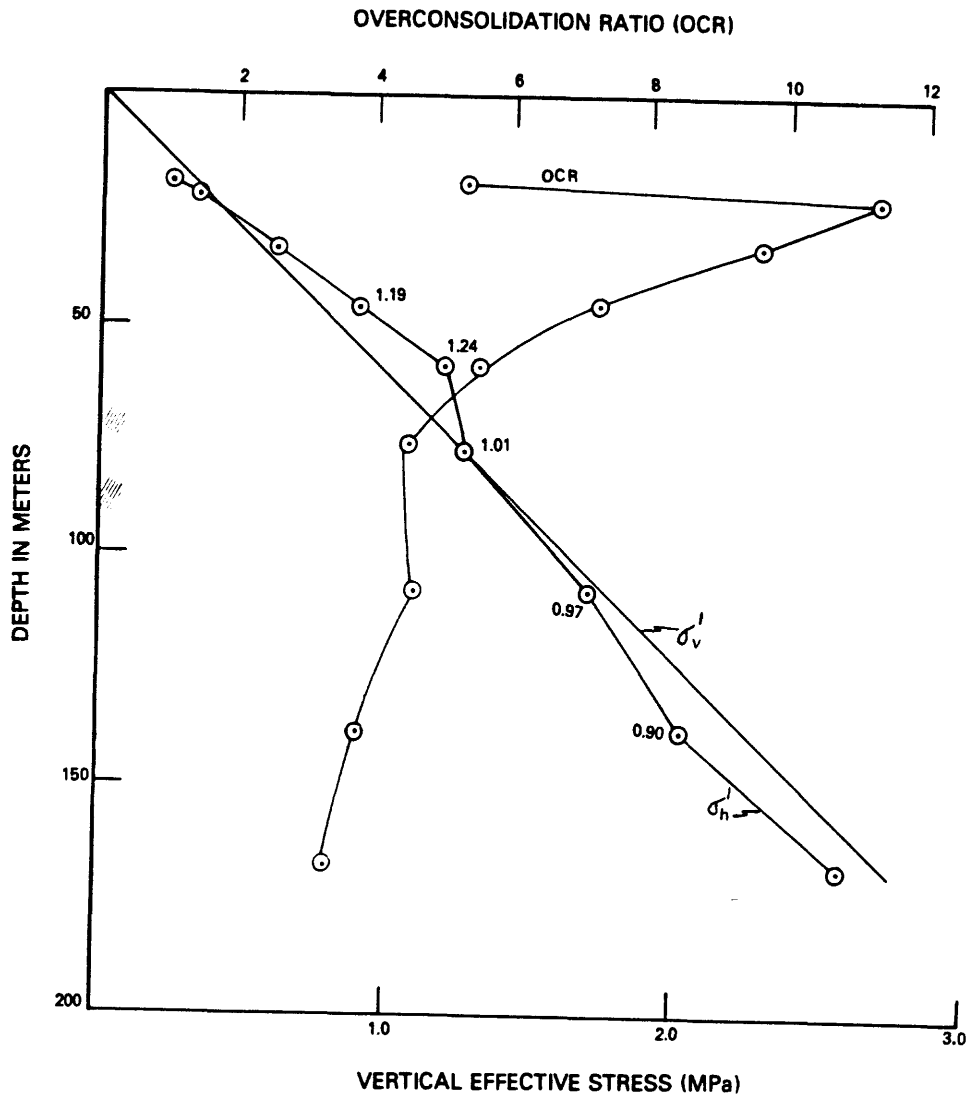

Figure 4.--Plots of horizontal and vertical effective stress ($'_h$ and $'_r$) overconsolidation ratio (OCR) with depth in hole H13. Hachures show location of fracture zones in same hole. OCR and average $'_h$ values determined with pressuremeter measurements, whereas the $'_v$ curve was determined using in situ bulk-density measurements and depth. Numbers adjacent to points on $'_h$ curve are values of K_0.

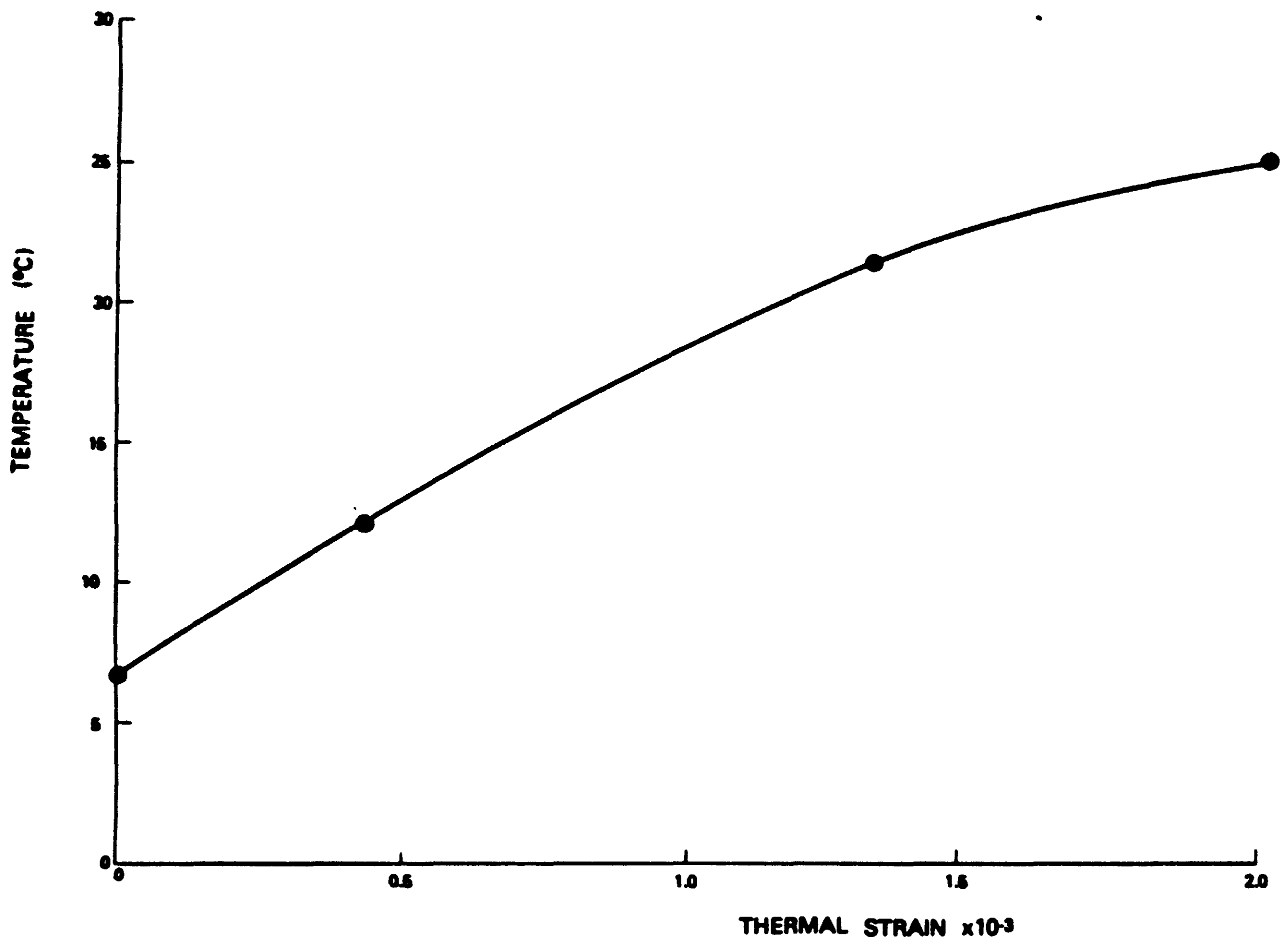

A

Figure 5.--Plot of thermal strain of two selected natural-state core samples. A, from 69.5-m depth and B, from 111.9-m depth in hole H12.

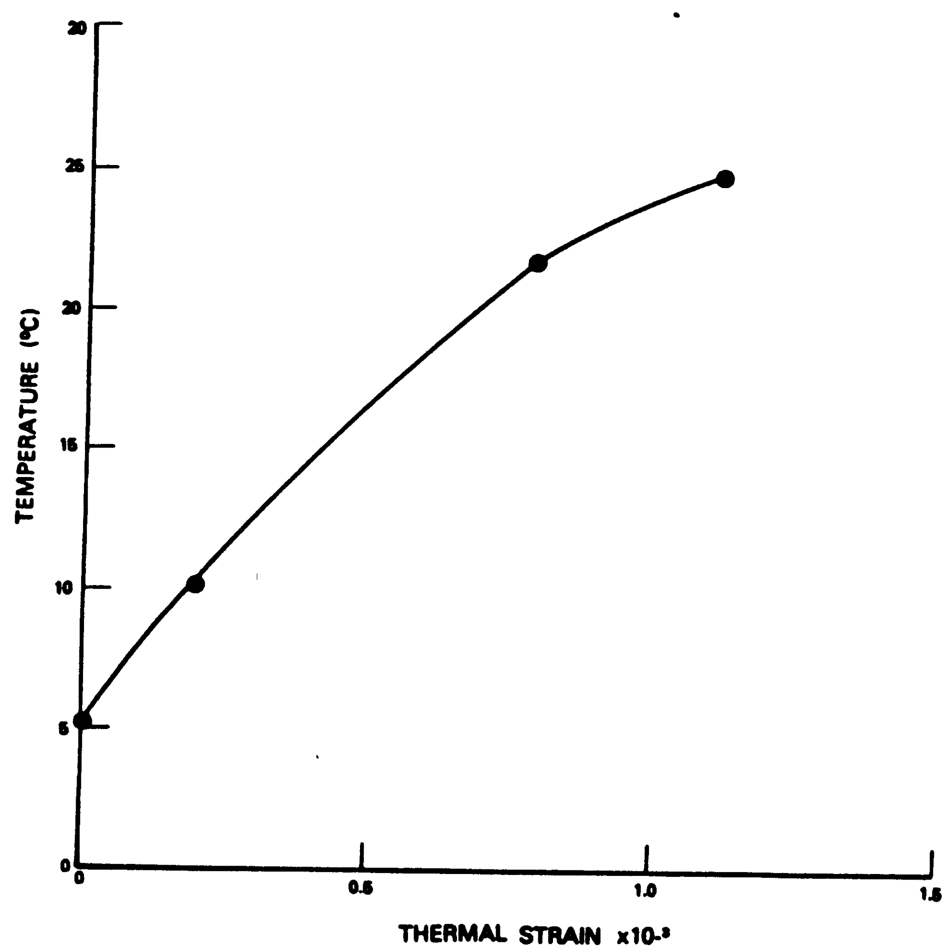

B

Figure 5.--Plot of thermal strain of two selected natural-state core samples. A, from 69.5-m depth and B, from 111.9-m depth in hole H12--Continued

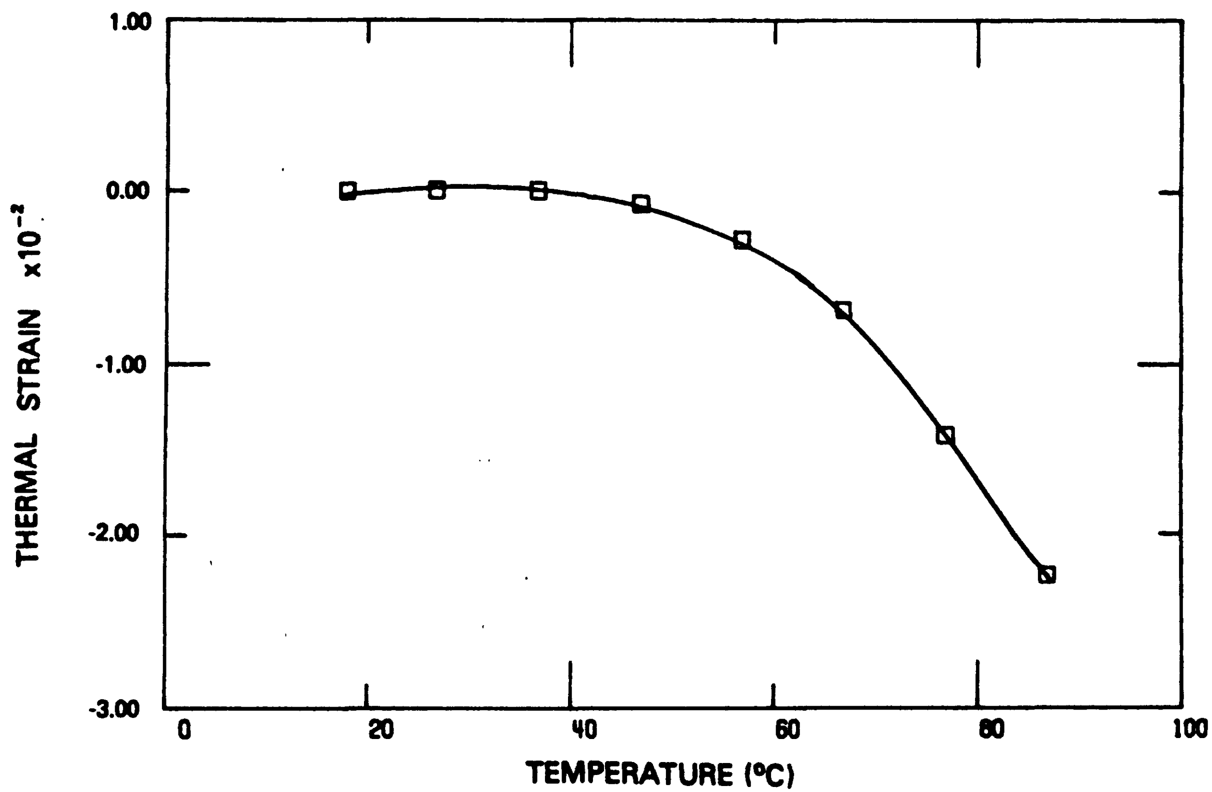

Figure 6.--Plot of thermal strain of selected sample from 63 m in hole H12. Sample was allowed to desiccate as testing progressed.

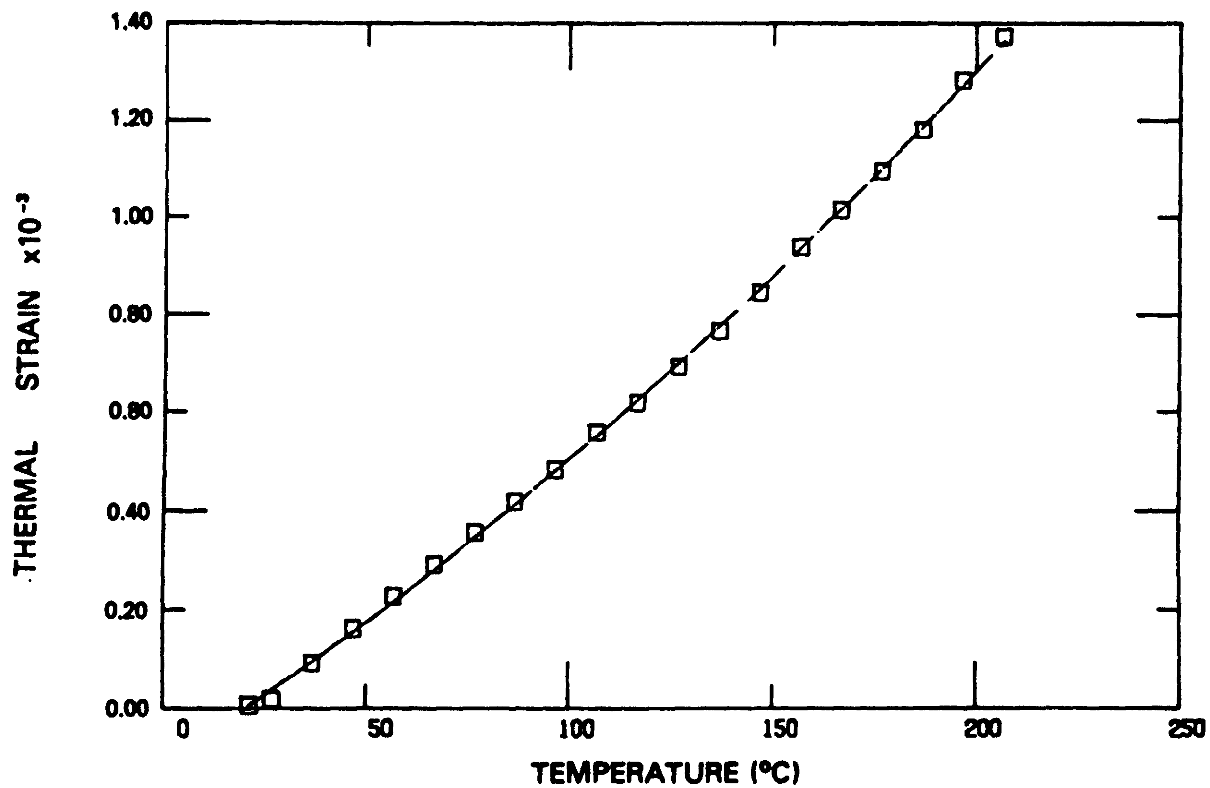

Figure 7.--Plot of thermal strain of desiccated sample used for figure 7.

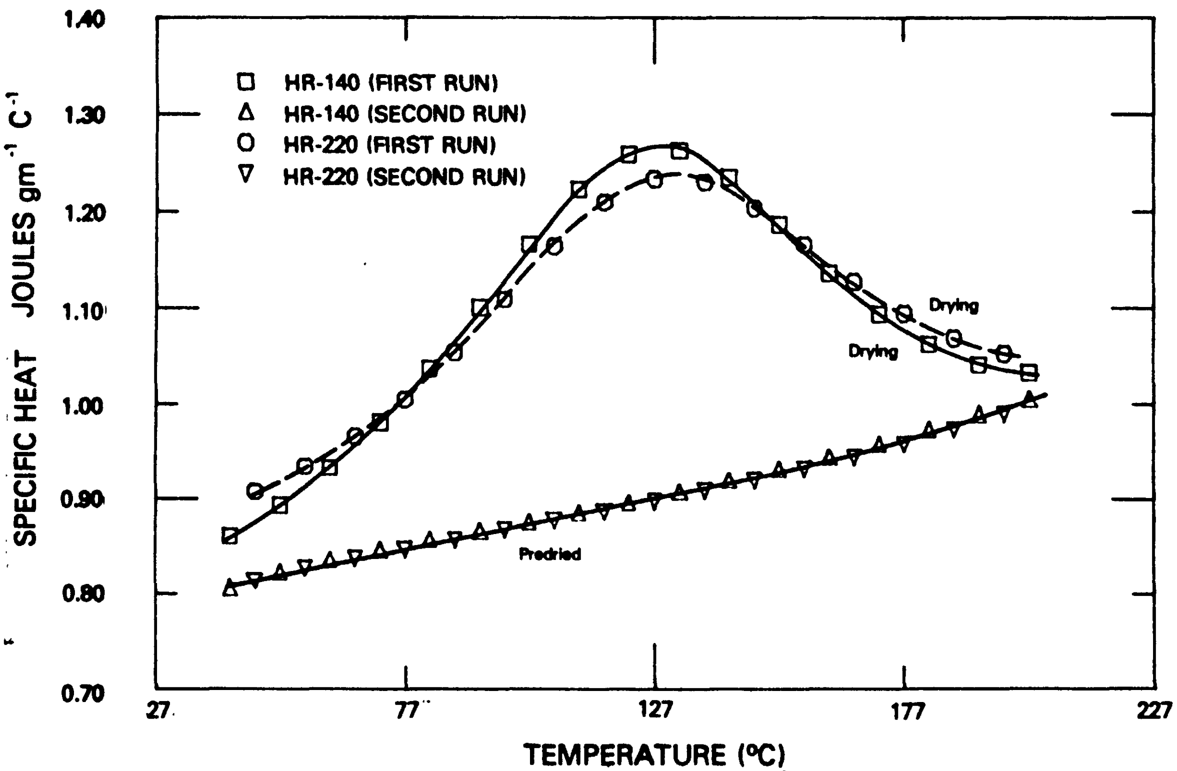

Figure 8.--Specific-heat measurements on selected cores from 43 m (HR-140) and 67 m (HR-22) in hole H12. First run: sample partially predried at 110° C; allowed to desiccate during test. Second run: sample desiccated prior to tests.

The thermal-properties data demonstrate that both the thermal coefficient of expansion and the specific heat change significantly as the sample is heated and moisture loss occurs. The conductivity of the shale appeared to be nearly uniform in all directions for natural-state cores. Conductivity in the desiccated cores was not determined, but desiccation of cores created dramatic changes in the other thermal and physical properties of the shale sufficient to cause serious problems in the interpretation of the thermomechanical deformations.

REBOUND

Rebound deformations of cores from holes H8, H10, H11, and H12 are shown in figure 9. The measurements were started on selected core samples within 30 minutes after they were removed from the borehole and were continued for at least 24 hours, and in some cases, up to 72 hours. Three measurements 120^{o} apart were made normal-to-core axes, and one measurement was made parallel-to-core axes. Initially, the cores were sealed so that during the measurements no measurable moisture losses occurred; therefore, deformations observed are not attributable to moisture changes. As can be seen by the data in figure 9, the most active rebound was observed in cores taken from holes H8, H10, and H11 from the 15- to 17-m-depth interval. In this interval, strains as much as 1.5 percent occurred, whereas, all other measurements show very little, if any, rebound.

Additional in situ creep and rebound data were obtained from borehole H13 at depths of 77, 108, and 168 m. These data were obtained with a pressuremeter by pressuring the shale to various levels and subsequently monitoring borehole deformations. Initially, pressures greater than overburden were applied for time intervals less than 1 hour; then pressures less than overburden were applied at two depths, 77 and 108 m, for about 13 hours (fig. 10). For the pressures greater than overburden, short-term outward strains as much as 0.4 percent were observed, and for pressures less than overburden, inward strains as much as 1.9 percent occurred. The largest strain (1.9 percent) occurred near a fracture zone.

SHEAR STRENGTH

Undrained triaxial compression tests were used to determine the average shear strengths of nine core samples taken at depths of 43-63 m in H8 (W. A. Braddock, written commun., 1982). The samples were deformed normal to bedding at strain rates of 10^{-5} to 10^{-7} per second under a confining pressure of 1.38 MPa (equivalent to 61 m of overburden). In addition, average shear strengths were calculated from published data of unconfined compression tests loaded normal to bedding, and direct shear tests sheared parallel to bedding (Fleming and others, 1970). The samples used to obtain these data were taken from very similar lithologies to those encountered in our sampling, but were recovered from core holes 48 km to the east. Finally, a profile of in situ shear strengths was developed from pressuremeter data obtained in hole H13 (R. Davidson, written commun., 1983). For comparison, these values are plotted in figure 11. The laboratory-determined triaxial test values are higher than pressuremeter values, but all values are relatively low compared to those of harder rock types. The laboratory direct-shear tests (Fleming and

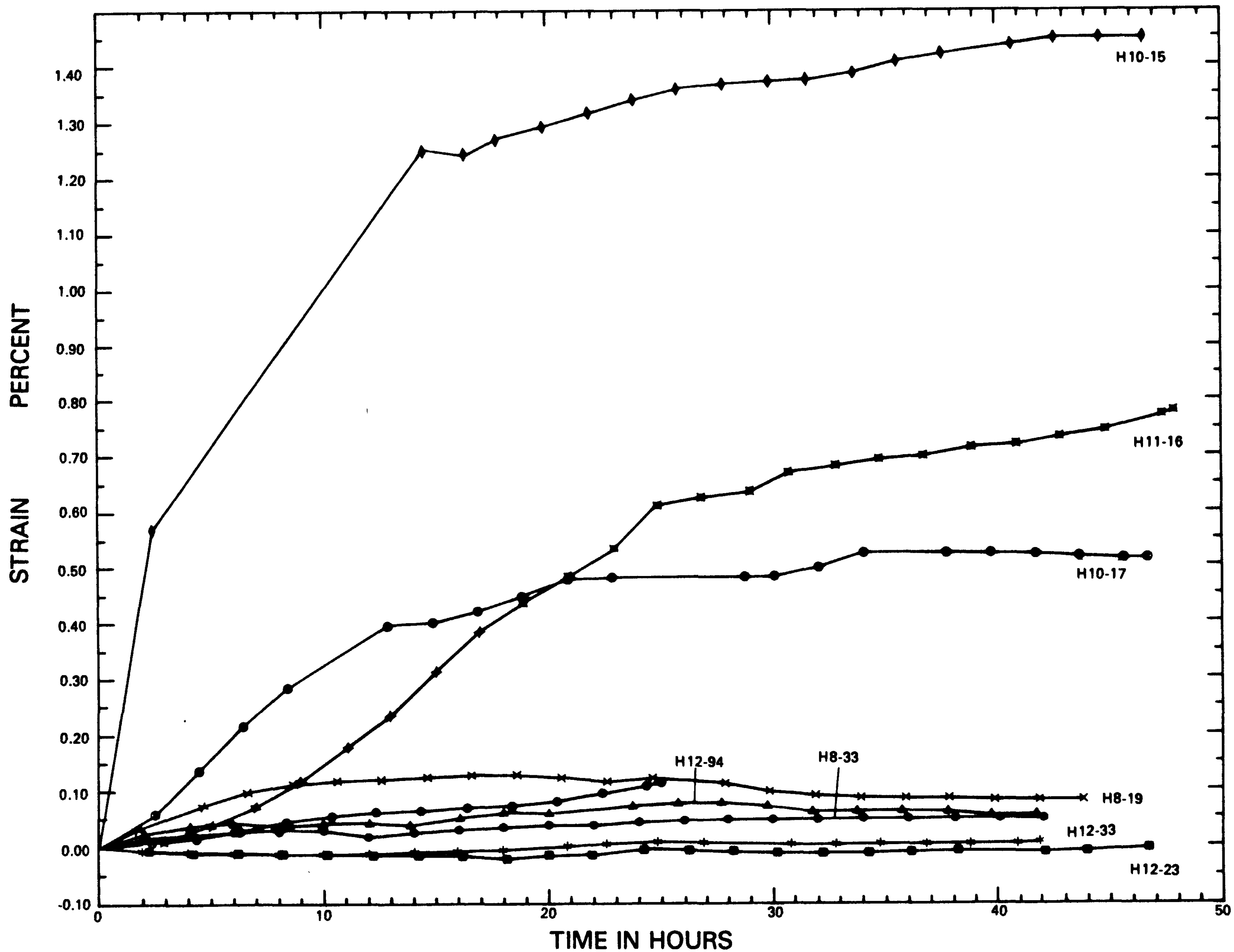

Figure 9.--Time-dependent vertical rebound of selected core samples from holes H8, H10, H11, and H12. Curve designations are hole number and depth in meters; that is, H10-17 is a core from hole H10 at a depth of 17 m.

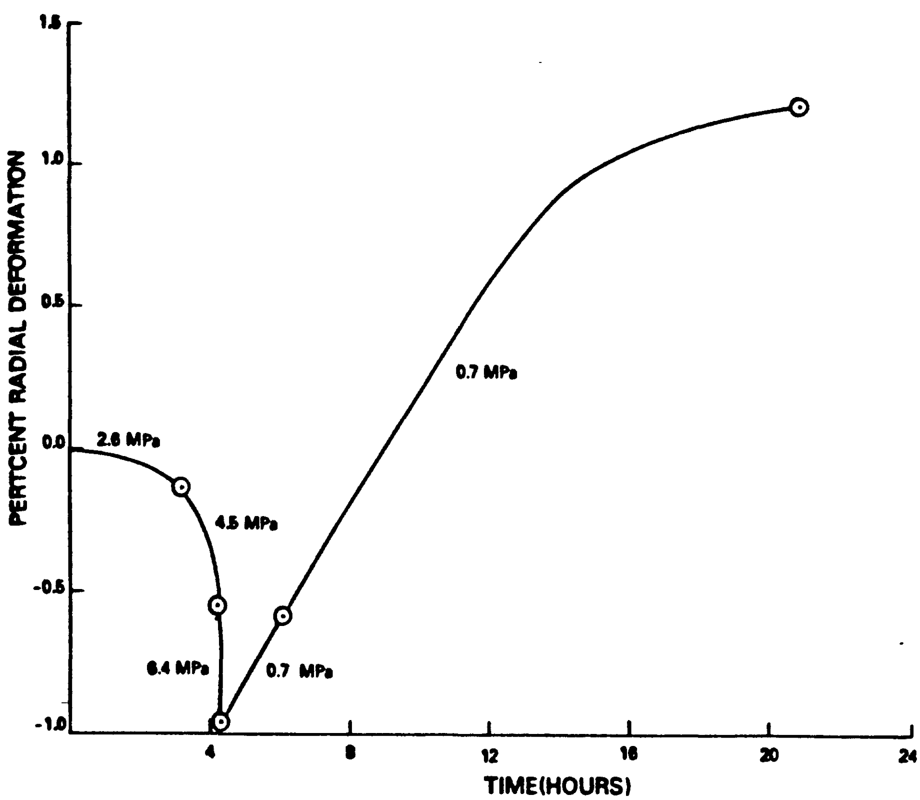

A

Figure 10.--Creep curves determined in situ with pressuremeter tests. Numbers show increments of pressure applied to borehole wall by pressuremeter. A, shows tests at 77 m and B, shows tests at 108 m in hole H13.

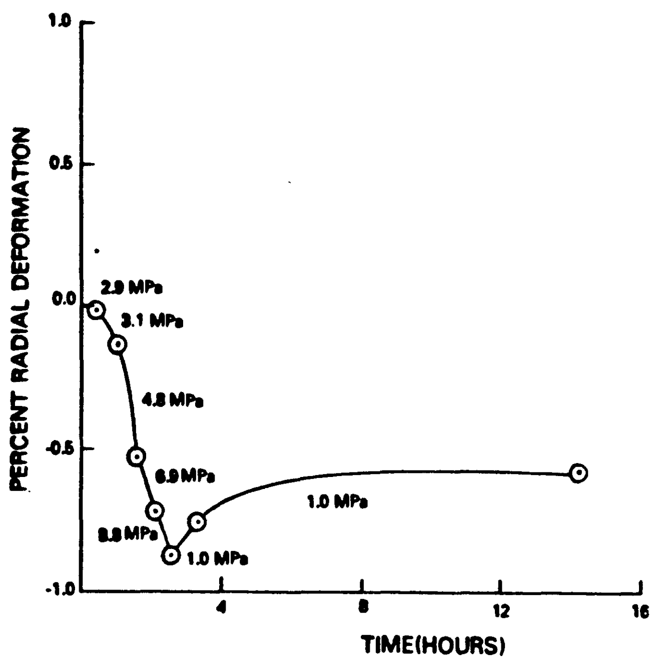

B

Figure 10.--Creep curves determined in situ with pressuremeter tests. Numbers show increments of pressure applied to borehole wall by pressuremeter. A, shows tests at 77 m and B, shows tests at 108 m in hole H13--Continued

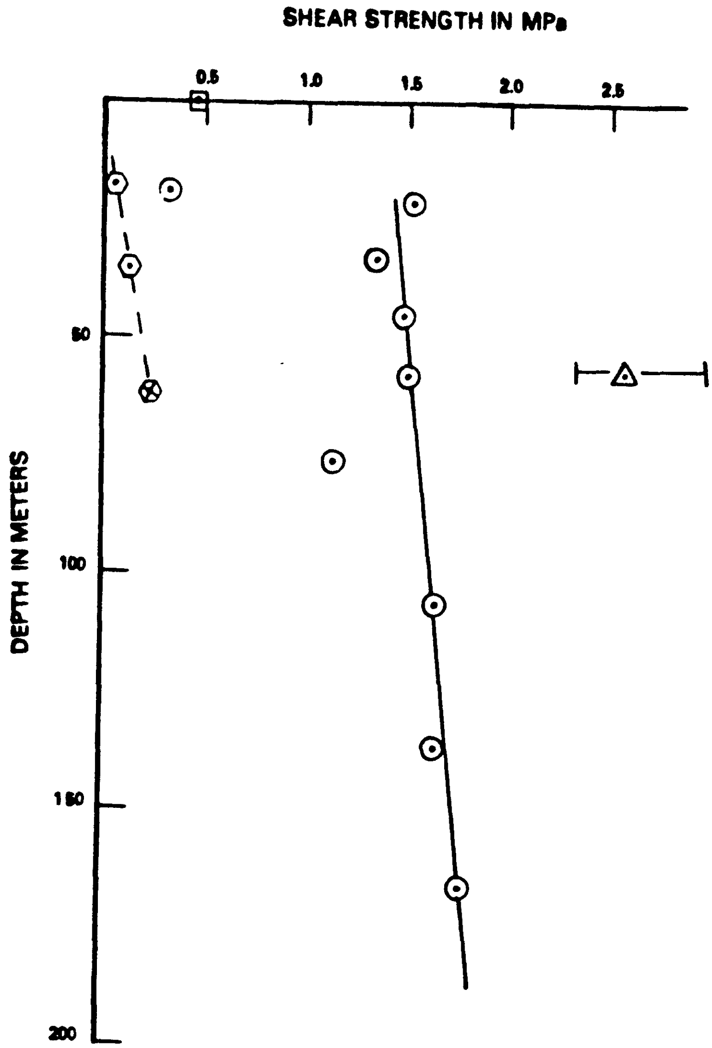

Figure 11.--Laboratory and in situ determined shear strengths versus depth. Average of nine triaxial shear strengths. △ , tests normal to bedding on samples from 43-63 m in hole H8. ⊙ , estimate of in situ shear strength determined from pressuremeter tests parallel to bedding in hole H13. ⊡ , average shear strength; unconfined compression tests normal to bedding (taken from Fleming and others, 1970). ⬡ , peak shear strength based on direct shear tests parallel to bedding (taken from Fleming and others, 1970). ⊗ , projected peak shear strength based on direct shear tests (taken from Fleming and others, 1970).

others, 1970) were performed parallel to bedding planes on samples taken from between bentonite beds that show significantly lower peak shear strengths than the triaxial and in situ pressuremeter test results.

PRINCIPAL CONCLUSIONS

The Pierre Shale, to a depth of 183 m, near Hayes, S. Dak., is a compact, dense, overconsolidated, smectitic, saturated clay shale. The shale is softer than most rocks and has a strong mechanical anisotropy perpendicular and parallel to the horizontal bedding. Upon heating, drastic changes of volume, strength, structure, moisture content, and thermal properties occur as the shale desiccates.

The in situ state of stress within the Pierre Shale was determined to be nearly lithostatic. With increasing overconsolidation toward the surface of erosion, horizontal stresses become slightly greater than the vertical stresses.

Rebound deformations can be significant from 15- to 17-m-depth intervals on undisturbed cores. Additional large time-dependent strains occur in borehole walls after being pressurized to values greater than overburden.

REFERENCES

Crandell, D. R., 1958 [1959], Geology of the Pierre area, South Dakota: U.S. Geological Survey Professional Paper 307, 83 p.

Davidson, R. R., 1979, Interpretation of the pressuremeter test: Woodward-Clyde Consultants Technical Memorandum 104-78, December.

Fleming, R. W., Spencer, G. S., and Banks, D. C., 1970, Empirical study of behavior of clay shale slopes: U.S. Army Engineer Nuclear Cratering Group, NCG Technical Report 15, v. 2, 304 p.

Neuzil, C. E., and Pollack, D. W., 1983, Erosional unloading and fluid pressures in hydraulically "tight" rocks: Journal of Geology, v. 91, no. 2, p. 179-193.

Sass, J. H., and Galanis, S. P., Jr., 1983, Temperatures, thermal conductivity, and heat flow from a well in the Pierre Shale near Hayes, South Dakota: U.S. Geological Survey Open-File Report 83-25, 10 p.

Tourtelot, H. A., 1962, Preliminary investigation of the geologic setting and chemical composition of the Pierre Shale and Great Plains region: U.S. Geological Survey Professional Paper 390, 74 p.